EXPERIMENTAL AND ANALYTICAL STUDIES OF CRYSTALLINE DAMAGE USEFUL FOR THE RECOGNITION OF IMPACT STRUCTURES

FRANK DACHILLE, PAUL GIGL, AND P. Y. SIMONS

Materials Research Laboratory and Department of Geochemistry and Mineralogy, The Pennsylvania State University, University Park, Pennsylvania

Large-scale effects of high-energy impacts have their counterparts in individual mineral crystals within the affected masses. Minerals of great stability preserve a record, decipherable by x-ray and optical methods, which may outlast grosser deformational features of the impact site.

X-ray methods can reveal internal fragmentation of crystals subjected to shock by the degree of asterism of the characteristic diffraction spots. For this study, and for the detection of high pressure phases, it is most practical to use the Debye-Scherrer technique with a single crystal (0.05–0.10 mm) rotated in the beam. Specimen crystals of quartz, calcite, and other minerals were examined from shatter cones, meteorite craters, volcanic and metamorphic rocks, atomic and chemical explosion sites, and elsewhere. Of special interest is the discovery of coesite in samples from the Sedan nuclear cratering event. Also examined were compacted powders of quartz and other minerals subjected to pressures of up to 120 kb at various strain rates in an opposed-anvil apparatus. The asterism-pressure relations found were comparable to those of granite samples from the Hardhat nuclear event, taken from known pressure zones.

Where the original location of a sample in the impact structure is not known, the asterism may be compared directly with that of samples ranging from undisturbed crystals to massively shocked ones. On a log–log plot of asterism vs. the asterism/line breadth ratio, a linear trend is obtained which is almost identical for both carbonate minerals and quartz. Volcanic and metamorphic samples give low values, while crystals from shatter cones or from shocked rocks have higher values, covering over two orders of magnitude.

An optical method for recognizing rocks subjected to shock processes is based on measurements of the spread of the optic axes of individual fragments of damaged single crystals. A Schmidt net plot of the fragment poles of a crystal provides a measure of its disruption. Averaged over 25 to 50 grains, the spread is greater for samples from meteoritic craters or explosion sites than for those from typical metamorphic, volcanic or undisturbed environments.

Observations made of light scattering from various rock specimens and single grains under illumination by a low intensity gas laser beam may have bearing on the reflective properties of the lunar surface.

INTRODUCTION

This conference on shock metamorphism attests to an expanding recognition of cosmic collision as a significant geological process. Investigations in this field are concerned with structures ranging in size from craters ($\leq$500 km) through large masses of chaotic breccia and individual shatter cones and down to individual lamellae less than a micron wide in discrete mineral grains. Some 12 orders of magnitude in linear dimensions are thus covered in such investigations, using visual methods from telescopic to microscopic. This work represents an extension to even lower limits of observation, by the use of x-ray and other methods to investigate small-scale structural effects which may be characteristic of high-energy impact processes.

Many lines of evidence are needed to detect or confirm remaining traces of meteorite impacts. Both the large structural features of craters, and even the metastable high-pressure phases of silica so useful as "index" minerals, are subject to erasure and alteration (Skinner and Fahey, 1963; Dachille, Zeto, and Roy, 1963; Gigl and Dachille, 1967). The effectiveness of these alteration processes is emphasized by the fact that, although about one million crater-forming impacts are

TABLE I

Sources of the minerals used in x-ray studies

Structure and locality	Rock type	Mineral studied
Meteorite impact craters		
Ries Kessel, Germany	suevite	quartz
Meteor Crater, Arizona	Coconino ss.	quartz
Steinheim basin, Germany	limestone	calcite
Wabar, Arabia	sandstone	quartz
Odessa, Texas	sandstone	quartz
Holleford, Canada	granite	quartz
Explosions		
Nuclear; Bonanza King Formation, Nevada	limestone	calcite
Nuclear; Hardhat Shot, Nevada	granodiorite	quartz
Nuclear; 100 kton-Sedan	granite	quartz
High Explosive (1000 lbs. TNT)	sandstone	quartz
Shatter cones ("crytoexplosion" structures)		
Decaturville, Missouri	limestone	dolomite
Wells Creek, Tennessee	limestone	dolomite
Sudbury, Canada	quartzite	feldspar
Sudbury, Canada	quartzite	quartz
Sierra Madera, Texas	sandstone	quartz
Steinheim basin, Germany	limestone	quartz
Vredefort, Africa	sandstone	quartz
Kentland, Indiana	sandstone	quartz
Metamorphics		
Nottingham, Pennsylvania	chlorite-magnetite mica-phyllite	quartz
Pilar, Norway	Metaquartzite	quartz
Arendale, Pennsylvania	biotite granite gneiss	quartz
Baker, Pennsylvania	phlogopite-tremolite marble	calcite
Pomeroy, Pennsylvania	marble	calcite
Volcanics		
Mt. Shasta, USA	volcanic bomb	quartz
Ubehebe Crater, California	volcanic bomb	quartz
Little Glass Mt., California	volcanic bomb	quartz
Mono Craters, California	pumice	quartz
Single crystals		
Large, euhedral crystals, source unknown:		
4 inches	natural quartz crystal	
2 inches	natural calcite crystal	

estimated (Dachille, 1962) to have been sustained by the Earth during its history, the number of structures which have even been considered to be of impact origin is presently under 120 (O'Connell, 1965; Freeberg, 1966). The number of accepted impact craters or possible craters actively being studied at this time is only about 50. Even at the optimistic rate of one crater discovery per month, only a small gain will be made, even in several centuries, in accumulating evidence of large numbers of catastrophic impacts. It is to be expected that, with time, more evidence will have to be sought at the lower end of the structural dimension scale, thereby placing increasing emphasis on microscopic and x-ray methods in the study of rock specimens and of individual crystals.

SCOPE OF THE STUDY

The conversion of the energy and momentum of a cosmic impact sets up, among other things,

a gradient of pressures from many megabars down to less than one kilobar and of temperatures from about 0.5×10^6 °K to ambient. Along these gradients, the structural integrity of single crystals is modified but may not be completely destroyed. Because of the unusual intensity and very short duration of impacts, the response of crystalline material might be expected to be characteristically different from effects imposed by normal metamorphic processes.

Unusual differences were sought in single crystals by using (a) single crystal x-ray diffraction methods to detect disruption of crystalline order and (b) microscopic observations of scattering of optic axes of subgrain fragments or of strained portions within disturbed single crystals. Observations were also made of the light-scattering properties of various rock specimens and single grains under illumination by a laser beam.

The samples investigated came both from accepted impact craters and from other non-impact environments, in order to provide specimens from a diversity of metamorphic and non-metamorphic conditions. Specimens included material from chemical and atomic explosions, volcanic bombs, slickensides, shatter cones, and fracture cones (Table 1 lists the materials used in the x-ray studies).

In addition, deformation effects were produced in polycrystalline compacts and cemented wafers during high-pressure experiments which employed opposed-anvil apparatus to simulate quasi-shock conditions.

X-RAY DIFFRACTION STUDIES

The x-ray procedures used were first described by Dachille, Meagher, and Vand (1964). Typical grains or single crystals are selected from rock samples, preferably from freshly-broken, unweathered surfaces. Under a binocular microscope, grains 0.05 to 0.1 mm in diameter are mounted on the end of fine glass fibers, and then examined in an immersion cell with a petrographic microscope in order to select those which appear to be single crystals. Such grains are then mounted in 114.6-mm diameter Debye–Scherrer x-ray diffraction cameras and exposed to Ni-filtered CuKα radiation, or to other wavelengths if necessary. The specimen is rotated during exposure.

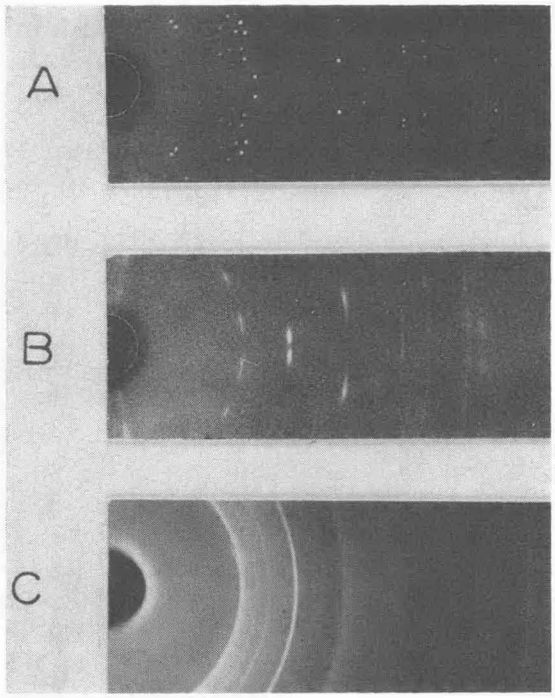

Fig. 1. X-ray diffraction spot pattern obtained from a small, undistorted crystal of beryl (A), contrasted with elongated spots of a deformed single zircon crystal in a sample from Ries, Germany (B), and with the "powder arc" pattern of a small crystal of albite, also from the Ries (C).

The resulting x-ray diffraction photographs reveal the relative perfection of these crystals. A good single crystal will yield a pattern of typical rounded spots, a mildly disturbed one will produce diffraction spots with varying degrees of elongation (asterism) and a highly shocked "single crystal" will yield arcs characteristic of powder patterns (Fig. 1). A critical point is that these types of patterns are all obtained from individual grains 0.1 mm or smaller in size.

Certain minerals may be more difficult to use than others for demonstrating differences in crystalline damage because of individual peculiarities of structure or because of very fine grain size. However, even micas, whose layered structure produces patterns indicating a high degree of orientation and curvature of lattice planes, can demonstrate effects of shock damage.

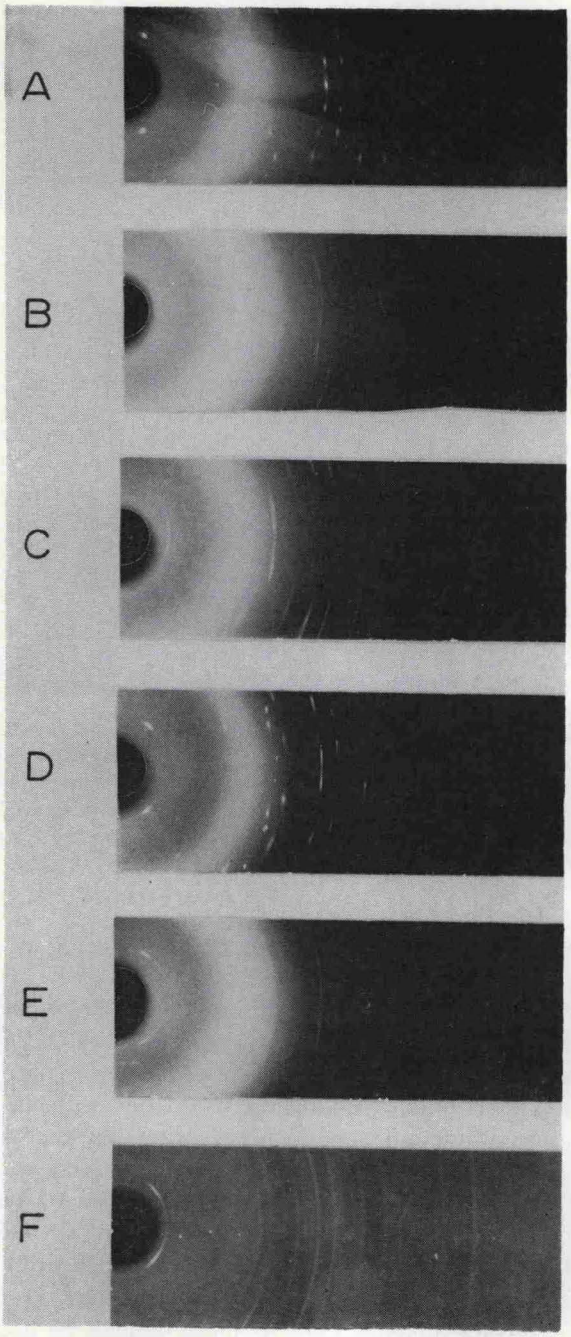

Fig. 2. "Single crystal" x-ray diffraction patterns obtained from micas; (A) typical, undeformed; (B), (C), (D), and (E), artificially subjected to 30 kb, 60 kb, 90 kb, and 120 kb respectively (see text); (F), a Ries, Germany sample.

In Figure 2, photographs (A) and (F) contrast patterns obtained from a small crystal of mica from an igneous rock (actually a "book" of crystals) with that of a mica crystal from a specimen of shocked rock from the Ries crater, Germany.

Limestones and dolomites are usually made up of very fine crystals, too small for normal use as indicated above. With such materials, small grains of equal volume can be used to provide roughly comparable patterns. In Figure 3, the diffraction pattern obtained from a limestone (A) and from the surface of a fracture cone formed in this limestone by dynamite during quarrying operations (B) are contrasted with the diffraction pattern of a grain from a shatter cone from the Steinheim Basin, Germany (C). It is apparent that the relatively mild quarrying explosion has served to break up and disorient the calcite crystals, but not to the extent indicated by the smooth, homogeneous arcs of the Steinheim sample.

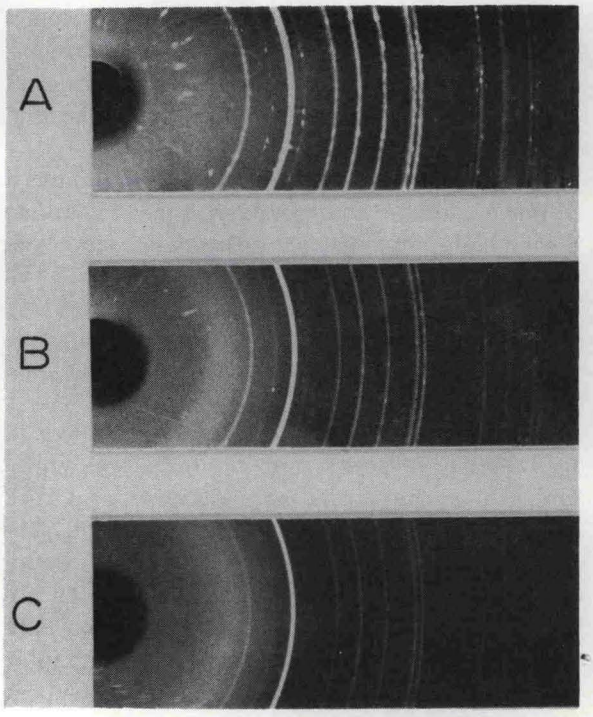

Fig. 3. X-ray diffraction patterns obtained from small grains of limestone from: (A) Trenton ls.; (B) Trenton ls. fracture cone; (C) Steinheim Basin shatter cone.

Quartz is perhaps the most useful mineral in the recognition of impact structures, because of its abundance, distribution, and durability, together with the fact that, in impact structures, it is the major host for the high-pressure minerals coesite and stishovite (Chao *et al.*, 1960, 1962). Figure 4 shows typical patterns obtained from quartz shocked by high explosives and by the impact which formed Meteor Crater, Arizona. In Figure 4C are seen the strongly "asterized" spots of the host quartz crystal as well as fainter powder arcs of coesite formed by the shock. A greater amount of coesite apparently occurs in the more severely deformed quartz crystal (Fig. 4D). The severity of asterism produced by the impact is remarkable.

Asterism is defined by Guinier (1952, p. 192–194) as the solid angle within which the normals to a family of lattice planes of a single crystal are to be found after deformation. The solid angle containing plane normals from the mosaic blocks of perfect single crystals is small, and a small spot is therefore produced on the film. As this solid angle increases, because of deformation or fragmentation, the diffraction spot becomes larger, and, in Debye–Scherrer geometry, the diffracted spot becomes longer along an arc of constant 2θ. It is this length which provides a measure of asterism.

Consider now a crystal of constant volume: the more numerous are the blocks into which it has been broken, the more chance there is for *any*, and *every* set of plane normals to describe large solid angles. This effect, together with the effects of specimen rotation and multiplicity of reflections, causes the scattered diffraction spots to merge and to produce a typical "powder arc" pattern as block sizes approach the lower limit still capable of diffraction.

Asterism in single-crystal diffraction patterns is usually associated, not with the Debye–Scherrer method, but with the Laue method of diffraction. Metallurgists have used the latter for decades to study deformation in metals. Bailey *et al.* (1958) used the Laue method in a study of polygonization in quartz; using the same method, we have also found diffraction effects consistent with those which they reported. However, we have emphasized the Debye–Scherrer technique for the following reasons:

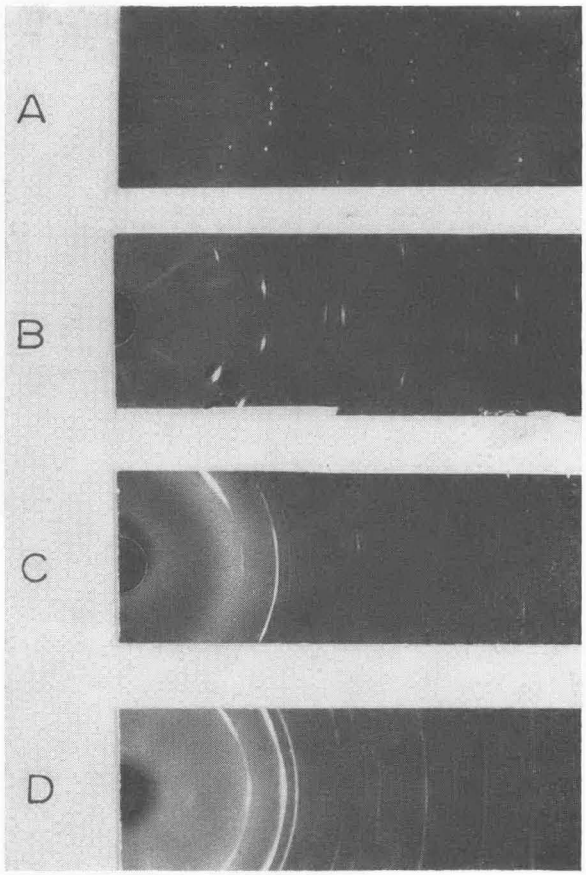

Fig. 4. X-ray diffraction patterns of quartz crystals: (A) typical, undeformed; (B) subjected to 1000 lb. TNT blast; (C) and (D), from Coconino sandstone, Meteor Crater, Arizona. Notice, in (C) and (D), the complete powder arcs of coesite (just to right of the strongest quartz reflection) associated with pronounced asterism of the quartz.

(1) It is simpler and faster, since exact orientation of the specimen is not necessary. Grains from many shocked rocks are small and anhedral, and many have indefinite crystal orientations under polarised light.

(2) Our primary aim was to detect and to qualitatively compare the extent of internal deformation in crystals, but not to investigate in detail the complex mechanisms inducing rupture of crystals within aggregates under shock conditions. However, study of specific mechanisms of

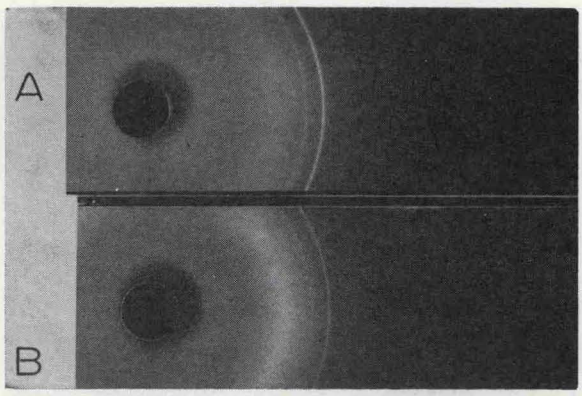

Fig. 5. X-ray diffraction patterns of coesite, identified in single grains in a specimen of shocked rock collected as ejecta from the Sedan nuclear cratering event (A, upper) compared with synthetic coesite (B, lower). In addition to the two strong reflections, there is good agreement with several weaker reflections that are clearly evident in the original films.

shock damage, using carefully controlled materials and conditions, may be facilitated with the use of the Laue method.

(3) The Debye–Scherrer method is highly effective for identification of minerals and also makes possible a sensitive scanning of host crystals for the presence of minor amounts of polymorphs or alteration products formed as a consequence of shock.

This last advantage is demonstrated by our detection of coesite in rocks from the Sedan nuclear event. To our knowledge, this is the first positive identification of coesite at the site of a nuclear explosion (Short, 1965).[1] We could not find the mineral by microscopic examination of thin sections or grain mounts, nor was it observed by standard x-ray powder diffraction methods of powdered bulk sample.

The coesite was found in a portion of the surface of the rock specimen which was finely crushed and compacted to a depth of about 2 mm. Most of this material was white and "sugary," but included a few scattered grains having a pale orange color. The latter amounted to about 0.1 volume percent. Under the microscope, both the white and orange grains appeared to consist of highly compacted, very fine fragments. Very few of the grains were transparent. Coesite was found only in the orange colored grains by means of the "single crystal" x-ray diffraction method. The diffraction patterns obtained are identical with that of a powder of coesite prepared in this laboratory (Fig. 5). The white grains gave diffraction patterns characteristic of "glass" or of polycrystalline quartz (with traces of unidentified minerals). By emission spectroscopy it was found that the white and orange grains did not differ noticeably in their elemental content.

No orange grains were found in the bulk of the sample which was very friable, although it had a granular texture similar to unaltered granite or granodiorite. The asterism of quartz crystals from the interior portion of the sample was pronounced, indicating exposure to severe shock.

It is suspected, from the appearance of the compacted portion of the surface and its relation to the bulk of the specimen, that the coesite was formed by the shock in a pre-existing fracture in the massive rock.

A second parameter useful in the assessment of damage sustained by crystalline materials is the width of the x-ray diffraction spot or line in the direction of 2θ. In a nominally "perfect" crystal, the blocks making up its mosaic structure are 2000 A to 20,000 A on edge. Theoretically, the width of diffraction spots from such crystals is of the order of 0.01 mm. However, because of the overlaid effects of sample, camera, and incident beam geometries, the actual width is closer to the 0.2 mm calculated for 500 A blocklets. Therefore, without rigid control of many factors, this method is not accurate for determining polygonization down to the 500 A range, and is even less so for blocklets of about 25 A or less. Although accuracy may be wanting, the procedure is sensitive enough to register spot broadening. It is noteworthy that, of hundreds of crystals examined, not one produced the very

[1] [*Editor's note.* Coesite has previously been identified in ejecta from the Scooter 500-ton conventional high explosive cratering test at the Nevada test site; it is estimated that peak pressures in this explosion reached 150 kb. (Milton, D. J., J. Littler, J. J. Fahey, and E. M. Shoemaker, Petrography of glassy ejecta from the Scooter 0.5-kiloton high-explosive cratering experiment, Nevada. *U.S. Geol. Survey Astrogeol. Studies Semiann. Progr. Rept., Feb. 26, 1961 to Aug. 24, 1961* (*March, 1962*), 88–92, 1962.]

diffuse spots indicative of domains 20 A to 100 A in size, and only a few specimens indicated domains of about 250 A to 350 A. Dependence of domain size on shock pressure might be expected (Dawson and Rose, 1963) and is the subject of further investigation. For the present, spot width measurements were made to compensate for the overriding effects of instrument geometry, sample size, and exposure time.

Inspection of the diffraction photographs obtained from natural and experimental samples of shocked and pressurized minerals reveals definite differences which make possible a relative grading of internal damage. Therefore, measurements of length of asterism and of line widths were made to provide relative numerical comparisons. All measurements were made directly from the films, using a low-powered microscope fitted with a calibrated micrometer scale whose smallest division was equal to 0.05 mm. Interpolation to 0.01 mm was possible, but because of gradation of contrast between the edge of the diffraction spots and background on the x-ray film, asterism and line breadth measurements were read with an estimated error of ± 0.025 mm. Since the average line breadth of diffraction spots was 0.25 mm, this value can be in error by ± 10 percent. Most of the asterism measurements, however, were over 1.0 mm, so that they can be in error by ± 2.5 percent or less. Because both asterism and line breadth are functions of the 2θ value, all measurements were made on the same 2θ values for a particular mineral. For quartz and calcite the diffraction maxima at 26.7° and 29.4° 2θ respectively (CuKα radiation) were used.

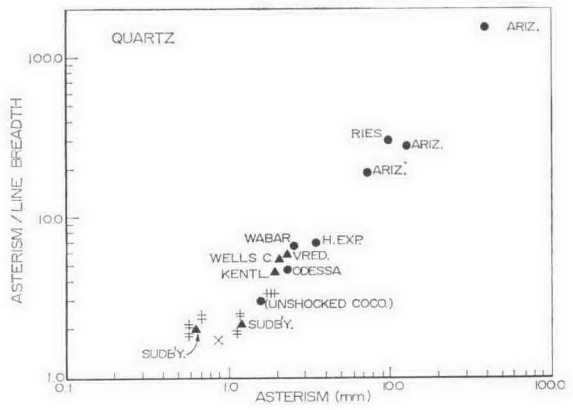

Fig. 6. Trend of the Asterism/Line Breadth ratio as a function of Asterism for quartz grains taken from various sources. The abbreviations refer to samples listed in Table 1. The symbols ‡, +, and × represent quartz grains from metamorphic, volcanic, and single crystal specimens respectively. Samples from shatter cones are indicated by triangles.

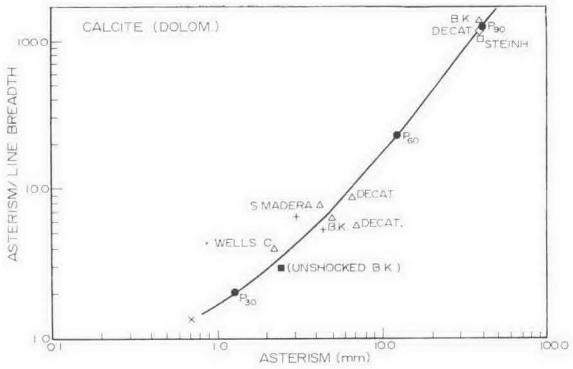

Fig. 7. Trend of Asterism/Line Breadth ratio as a function of Asterism for calcite samples from various sources. Superimposed on the diagram are data from pressure deformation experiments on calcite polycrystalline samples—(vide infra) to illustrate the range of pressure associated with the asterism observed. The abbreviations refer to samples listed in Table 1. The points marked P_{30}, P_{60}, and P_{90} are results obtained from subjecting powder compacts of calcite to pressures of 30 kb, 60 kb, and 90 kb, respectively, in an opposed anvil apparatus. The × refers to the measurements obtained from the pattern of a small undisturbed single crystal of calcite. Samples from shatter cones are indicated by triangles.

A summary of measurements for quartz and limestone samples is given in Figures 6 and 7, where the ratio, Asterism/Line Breadth, is plotted logarithmically against the Asterism (A/LB vs. A). The error in the Asterism/Line Breadth ratio is about ± 11 percent and is caused mainly by the error in line breadth measurements. The trend to higher values demonstrates increasing crystalline fragmentation in progressing from good single crystals to specimens from volcanic, metamorphic, shatter cone, and impact samples. There is some overlapping (in the region from 0.7 to 1.8 mm on the asterism scale) for samples from Sudbury, unshocked granite, Coconino sandstone, and samples of metamorphics. Nevertheless, the distribution of the asterism in minerals from shatter cones strongly suggests that the intensity of deformation is a result of cosmic impact.

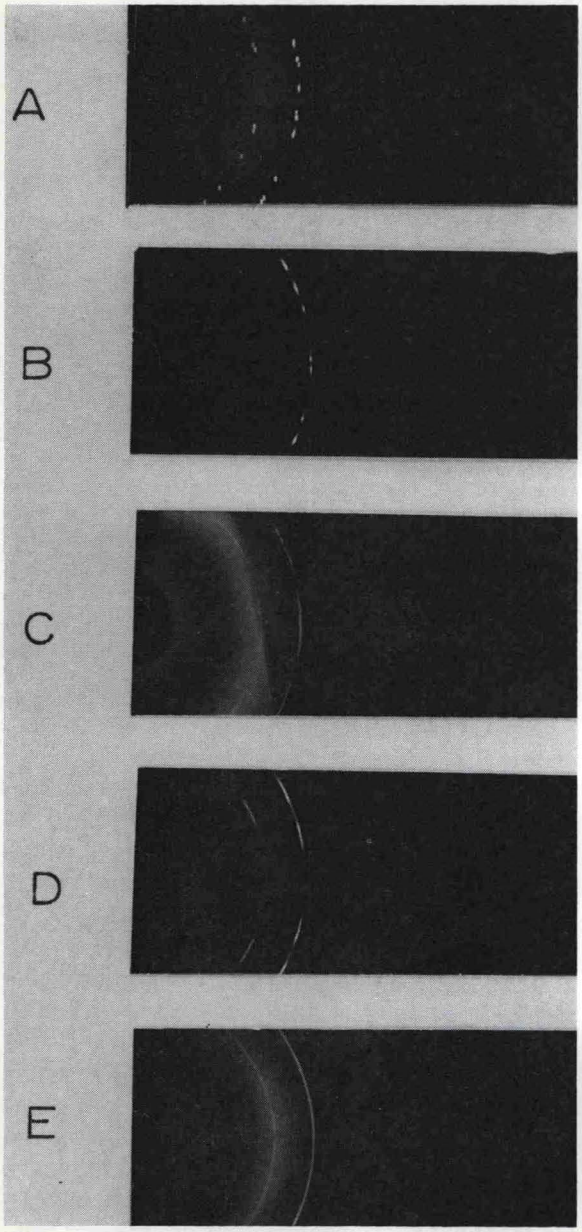

Fig. 8. Progressive asterism developed in quartz grains from polycrystalline compacts under increasing pressures: 10 kb (A), 40 kb (B), 90 kb (C), 100 kb (D), and 120 kb (E).

The following cautionary observations are pertinent: (1) The absolute values should be taken only as guides in forming conclusions. (2) The locations of the shatter cones relative to the centers of the structures from which they came are not known, and attempts to correlate the results with sizes of the structures are not possible. (3) The possibility of recrystallization of minerals after shattering and impact must be considered, e.g. for the older Sudbury and Vredefort samples. Disoriented overgrowths may contribute to apparent asterism of minerals in sediments. (4) The characteristics of minerals in the pre-impact host rocks of any suspected structure must be known. The normal quartz in unshocked Hardhat granodiorite and Coconino sandstone shows asterism close to that of some metamorphic rocks, but, after exposure to shock, there is a large increase in asterism. The initial asterism may have had its origin in the previous thermal and mechanical history of the rock or in the source area of original detrital grains.

QUASI-SHOCK HIGH PRESSURE EXPERIMENTS

To assist in evaluating the pressure dependence of asterism observed in shocked minerals, experiments were conducted in an opposed-anvil apparatus up to 120 kb pressure at room temperature. Apparatus and techniques have been developed in numerous studies over a period of ten years in this laboratory.

The minerals used in these experiments were quartz, calcite, albite, mica, and olivine. Materials were prepared by gently crushing large single crystals and using the fraction between 200 and 270 mesh. Each wafer was prepared by measuring the amount of powder necessary to fill, at theoretical density, the volume enclosed by the nickel ring of the apparatus (dimensions, 0.1875″ O.D.×0.125″ I.D.×0.01″ thick). A new sample was prepared for each pressure.

Three series of runs were made, one at a rate of 5 kb/minute, a second at a rate necessary to attain the required pressure in two minutes, and a third at 60 kb/minute. The latter rate was not wholly an arbitrary choice; it accomodated mechanical limitations and helped to reduce the frequency of shattering of anvils at the highest pressures.

Each sample was held at the required pressure for 5 minutes and then removed for examination. Grains were picked out of both the central and edge regions of the wafer and prepared for x-ray

diffraction examination. Typical patterns obtained are shown in Figures 2 (B, C, D, E), 8, and 9.

The increase in asterism with increasing pressure is evident, and the similarity to asterism found in shocked specimens is noteworthy (compare Fig. 8 and Fig. 4). Calcite and albite behaved similarly, but, at pressures above 90 kb, the crystals were fragmented into particles too small to be x-rayed effectively by this method. This fragmentation is attributed chiefly to cleavages in these minerals. Pressure experiments also were made using cut wafers of well-cemented Tuscarora quartzite and of mica.

Figure 10 shows the change in the Asterism/Line Breadth ratio with pressure observed for both quartz powder compacts and quartzite wafers. As expected, grains from the edge show a somewhat greater change, the reason being that, during compaction, these grains are displaced more than those at the center because of greater marginal shearing stresses. This result is consistent with the lower values obtained using wafers of Tuscarora quartzite, in which relative motion of grains is minimized by the tight cementation. Figure 10 also shows effects of varying rates of pressurization. Apparently, during rapid pressurization to about 60 kb, the deformation at grain contacts necessary to produce zero porosity in the wafer produces more local stress concentrations and asterism than are produced at slower pressurization rates. Above this pressure, the greatest part of the porosity has been eliminated, and relatively less lateral displacement, and less asterism, is caused by higher rates of pressurization.

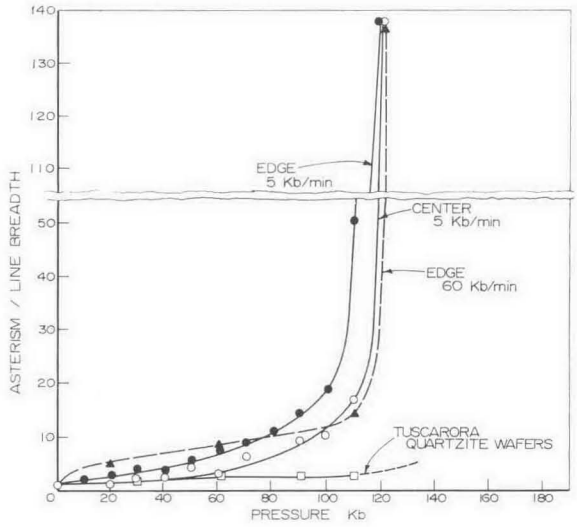

Fig. 10. Changes in Asterism/Line Breadth ratios of grains from polycrystalline quartz compacts and from well-cemented quartzite wafers as a function of applied pressure.

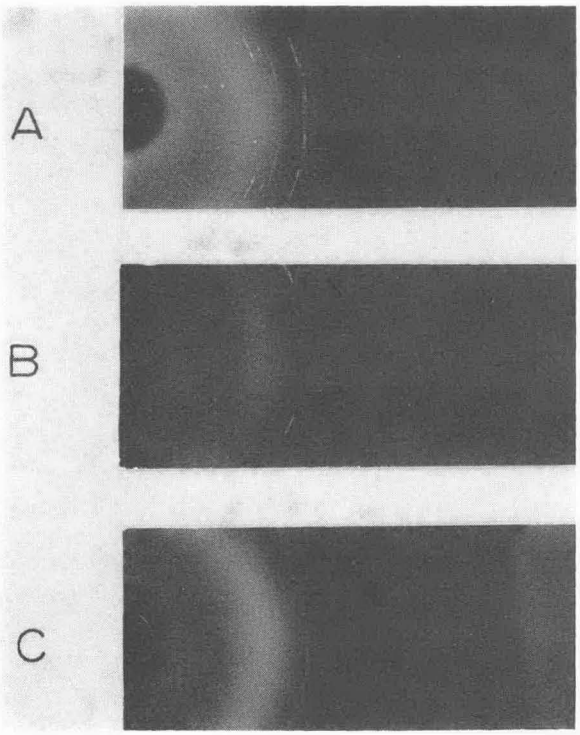

Fig. 9. Progressive asterism developed in albite grains from polycrystalline compacts with increasing pressures: 30 kb (A), 60 kb (B), 90 kb (C).

Results obtained for granodiorite samples from different pressure zones of the Hardhat nuclear explosion (Short, 1966) and from a granodiorite boulder subjected to more than 150 kb peak shock pressure during the Sedan cratering event are plotted in Figure 11. They illustrate the combined effects of competent rock types and of very high pressurization rates by their divergence from the opposed-anvil results.

Discussion of experimental work with opposed-anvil, high-pressure techniques never fails to raise remarks that, (1) the pressures are not "hydrostatic," (2) shear stresses may support very pro-

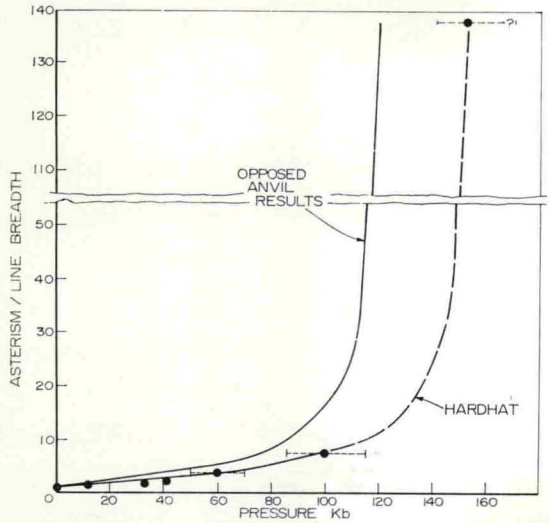

Fig. 11. Asterism/Line Breadth ratios from opposed-anvil pressurization experiments compared with data from material from known pressure zones of the Hardhat and Sedan nuclear explosions (Short, 1966). The horizontal dashed lines give the estimated pressure error (N. M. Short). The point plotted at 150 kbars is for the Sedan event for which the upper limit of pressure is not known. The other plotted points are for the Hardhat samples.

nounced pressure gradients in the samples, and (3) that shear stresses somehow change the reactions. This is hardly the place for an extended discussion of subjects which have been the concern of several high pressure conferences, but the following comments can be made. In no experimental system using bulk solid media to generate high pressures for solid state reactions can it be said that ideally hydrostatic conditions prevail. The problems of calibration of pressure against applied load are serious complications in all such apparatus. In any polycrystalline material, cemented or not, neither stress nor strain will be uniform on a grain-to-grain basis in the early stages of response to an applied force. This condition prevails in both opposed-anvil apparatus and in geological systems. As for pressure gradients in wafers, we are aware of this problem, having made studies for their control or elimination (Myers *et al.*, 1963).

The effect of shearing stresses on reactions has also been investigated in this laboratory (Dachille and Roy, 1964). The major findings are: (1) reaction rates are generally increased, probably through lowering of the activation energy in a shear stress system, (2) the increase in reaction rates is roughly equivalent to that which would be obtained by an increase of about 100° to 200°C in temperature, and (3) equilibria are not displaced significantly.

It may be concluded that the pressure history of an individual grain in a polycrystalline mass cannot be known in detail. The asterism in a crystal reflects the sum of all disturbing influences up to and during pressurization, and from the consistency evident in Figures 10 and 11, the sum is dependent on pressure. In Figure 12, the data for quartz from opposed-anvil and shock pressure experiments are plotted on the scale of Figure 6. The strong coincidence between experimental data and the measurements on natural samples indicates similarities in causes and effects. The scales constructed from the opposed-anvil and shock results allow some estimation of the approximate pressures of shock metamorphic processes.

Shock events in porous or poorly-cemented sandstones, tuffs, etc. will tend toward the values for opposed-anvil results, whereas events in strong, well-cemented rocks such as quartzites and granodiorites can be estimated from the Hardhat-Sedan data (Fig. 12). The comparatively low values for Sudbury shatter cone samples, aside from the possibility of recrystallization, may arise from the highly competent nature and great depth of the host rocks at the time of impact.

Figure 7 shows a comparison of results from opposed-anvil pressure experiments on calcite with values obtained from various limestone and shatter cone samples.

A comparison of the Asterism/Line Breadth values of crystals from the unaffected host formation and from a disturbed region in the host formation can be helpful in determining the nature and intensity of the disturbance. For example, the results of a dozen quartz crystals taken from Coconino sandstone outside Meteor Crater cluster close to the values $A/LB=2.1$ and $A=0.84$, whereas shocked quartz crystals from boreholes within the crater ranged to the upper limits of the scales. Similar relations were observed in samples of dolomite (Bonanza King

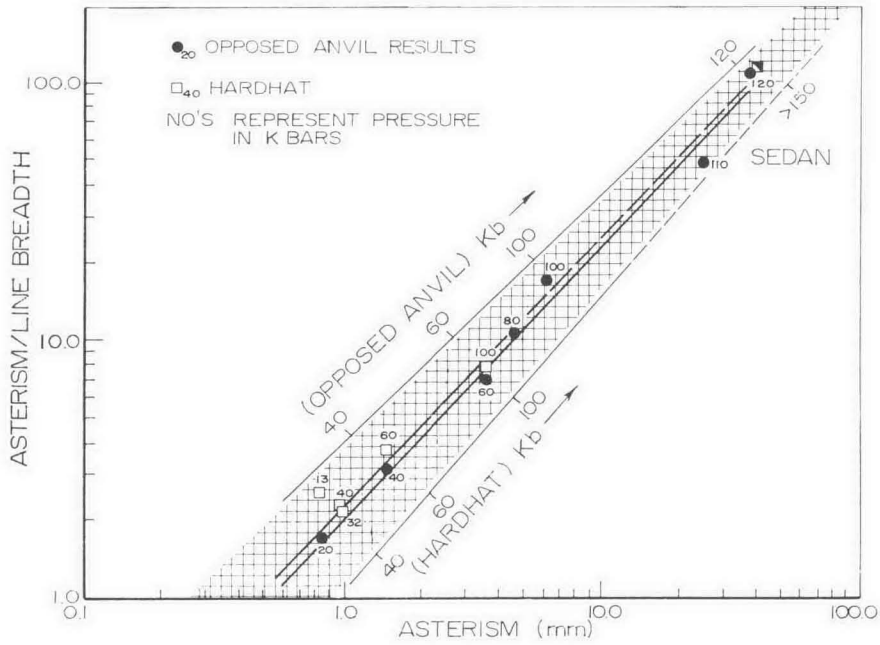

Fig. 12. Approximate but qualitatively useful relations between applied pressure and resultant asterism observed in quartz in "quasi-shock" studies with an opposed-anvil apparatus and in shock experiments.

formation) from the Handcar nuclear event. When undisturbed reference samples are not available, asterism values above 2.5 mm for single crystals of quartz should serve as an alert to the possibility that the rock has been subjected to impact. Numerous readings above this value would be highly indicative of a shock history unless obvious facts to the contrary are known.

OPTIC AXIS MEASUREMENTS IN THIN SECTION

Previously, we described how x-ray diffraction was used to demonstrate and evaluate the degree of scattering of plane normals of submicroscopic blocks which now compose crystals that have been subjected to deformation processes. In this section are discussed observations on a microscopic scale first reported by Dachille, Fauth and Vand (1964), of the scatter of optic axes of fragments or of distorted portions of single quartz crystals.

The optic axis measurements were made on standard thin sections, using a petrographic microscope with a four-axis universal stage. Initial measurements were made on specimens of typical unshocked and shocked Coconino sandstone from Meteor Crater, Arizona (the latter material, courtesy of E. M. Shoemaker). Results warranted extension of the study to other sandstones, to gneisses and quartzites from metamorphic terranes, and to material from other probable or actual meteorite impact areas.

For comparison, 25 grains obtained by selecting 5 grains along each of 5 equally-spaced traverses were measured in each sample. Optic axis orientations of only those grains whose diameter *exceeded 0.5 mm* were measured, in order to minimize the effects of uncertainties in readings, and to avoid small crystals in heterogeneous rocks which may have been shielded from pressure effects. Three measurements were made on crystals exhibiting continuous undulose extinction: as the extinction "wave" entered, passed the center, and left, the grain. On segmented crystals or on crystals with discontinuous undulose extinction (patchy extinction), the axis orientation of each segment or patch was determined.

Measurements were plotted on the lower hemisphere of a 20 cm diameter equal area net. Points plotted for each grain were enclosed by

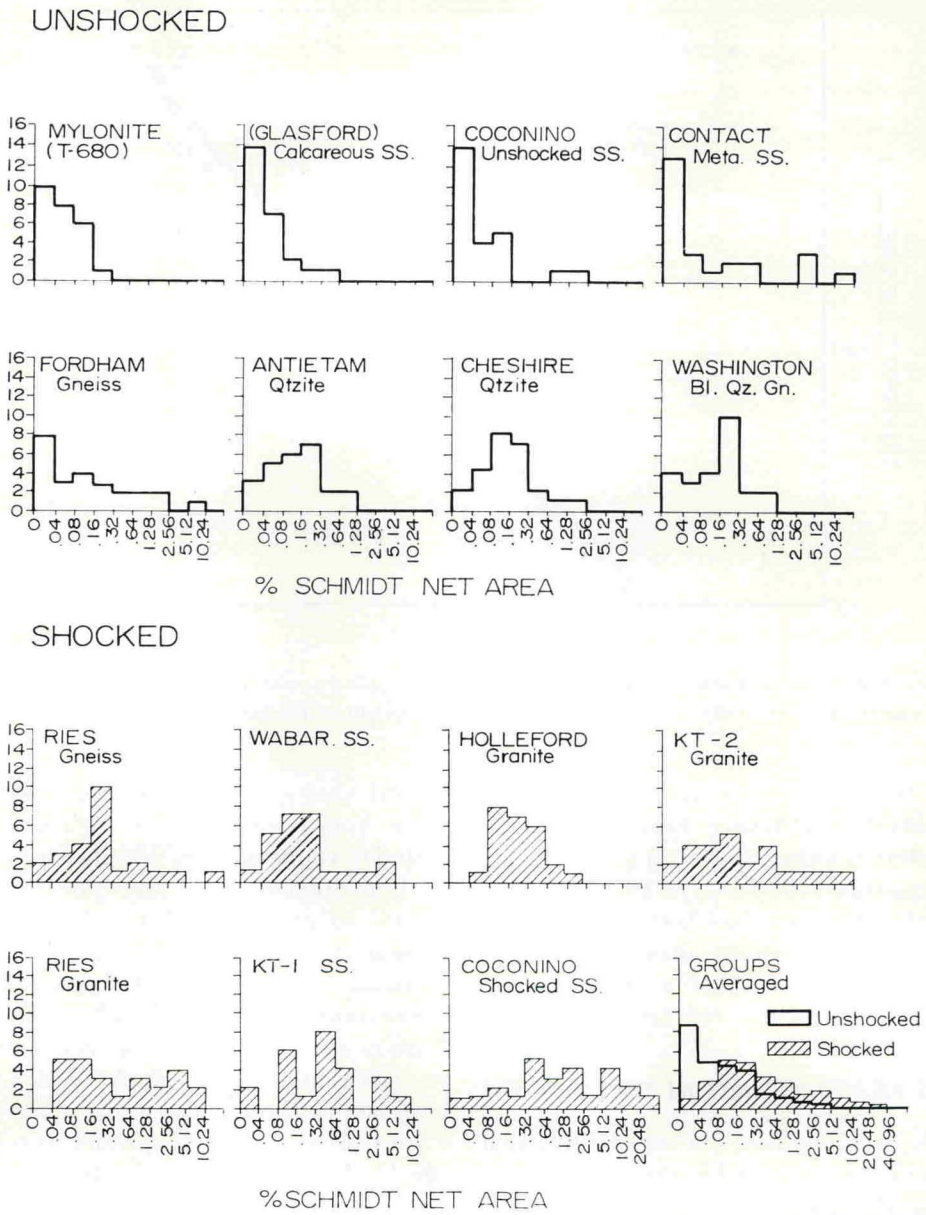

Fig. 13. Histograms which indicate some basic differences in distribution of areas of optic axis dispersal polygons of quartz crystals from both unshocked and shocked rocks. The size classes, in terms of percent of Schmidt net area, start with 0.04 to absorb basic errors of measurement. The averaged histograms in the last diagram emphasize the differences and show the smoothing to be expected from measuring a larger number of grains.

the smallest possible polygon, whose area is thus a measure of the dispersion of the optic axes produced by strain or fragmentation of the original grain. Of course, readings of grains exhibiting straight extinction plot as single points and therefore yield zero areas. For comparison of the shapes of the "dispersal" polygons, the center of each was rotated to the center of the net, but an analysis of these comparisons is not pursued in this report.

TABLE II

The relative ranking from largest to smallest values of optic axis dispersion by average, mode, and median values. The values are calculated on the basis of percentage of Schmidt net area of "dispersal" polygons determined by the optic axis measurements. See text for method.

Rank	By mode	By average percent of net area		By median percent of net area		By average rank
1	Shocked Coconino ss.	Sh. Coco. ss.	3.7	Sh. Coco. ss.	1.17	Sh. Coco. ss.
2	Ries granite	Ries gr.	1.5	KT-1 ss.	0.37	Ries gr.
3	100 KT-2 granite	KT-2 gr.	1.4	KT-2 gr.	0.27	KT-2 gr.
4	100 KT-1 sandstone	Con. meta. ss.	1.1	Ries gr.	0.21	KT-1 ss.
5	Antietam ss.	Ries gn.	0.98	Ries gn.	9.21	Ries gn.
6	Ries gneiss	KT-1 ss.	0.86	Holleford gr.	0.19	Wabar ss.
7	Washington Blue Quartz gneiss	Fordham gn.	0.57	*Wabar ss.*	0.19	*Holleford gr.*
8	Cheshire quartzite	Wabar ss.	0.48	Wash. B. Qtz. gn.	0.18	Wash. B. Qtz. gn.
9	Wabar ss.	*Holleford gr.*	0.35	Ches. qtzite	0.16	Ches. qtzite
10	*Holleford granite*	Ches. qtzite	0.25	Antietam ss.	0.14	Antietam ss.
11	Fordham gneiss	Wash. B. Qtz. gn.	0.22	Fordham gn.	0.10	Fordham gn.
12	Mylonite	Antietam ss.	0.19	Mylonite	0.05	Con. meta. ss.
13	Contact metamorphosed ss.	Unsh. Coco. ss.	0.14	Con. meta. ss.	0.04	Mylonite
14	Unshocked Coconino ss.	Glasf. cal. ss.	0.10	Unsh. Coco. ss.	0.04	Unsh. Coco. ss.
15	Glasford calcareous ss.	Mylonite	0.04	Glasf. cal. ss.	0.03	Glasf. cal. ss.

We are indebted to R. S. Dietz, C. P. Thornton, N. Short, E. M. Shoemaker, and T. E. Bunch for many of these samples.

The italics emphasizes the position of the lowest-ranked impact source in each category. The fourth column averages the rankings of the first three columns.

Frequency distributions based on an area size class for most of the sections measured are given in Figure 13. The histograms of the shocked specimens are skewed to higher area classes and are more spread out than are those of unshocked specimens. This characteristic is especially noticeable in the last histogram of the figure, which averages the histograms of the two groups and provides the smoothing effect to be expected from a larger number of readings. It would be difficult to decide on the basis of a single histogram of only 25 readings, such as that of the Cheshire quartzite, that the specimen had or had not been subjected to impact. However, by calculation of the average, mode, and median values, an almost perfect separation can be made between samples from impact and non-impact environments. The relative ranking from largest to smallest values of optic axis dispersion by the average, mode, and median values of the polygonal areas are shown in Table 2 for seven samples of impact origin and eight of non-impact origin. The fourth column averages the three rankings and supports the complete separation effected by the median values.

It should be mentioned that, as with the x-ray diffraction asterism findings, the relative ranking of the impact samples does not necessarily imply the same order of the intensity of the impact event, because the samples available were from random locations.

Gneisses and quartzites are difficult to separate from impacted rocks on the basis of the average and mode values; they also rank immediately below the median values of rocks displaying the mildest impact damage. The concentration into the small area classes of optic axis scatter of quartz grains from contact metamorphosed sandstone and mylonite is surprising in view of the impression of chaotic fragmentation seen in the thin sections. However, this difference is understandable in view of basic differences between these metamorphic processes and those of impact.

Thermal effects are essentially one-dimensional, in the direction of expansion or contraction, and

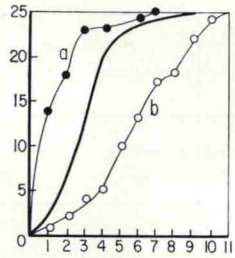

Fig. 14. A plot of the cumulative number of fractured or strained crystals of quartz whose optic axis dispersal polygons are equal to, or smaller than, the area specified on the abscissa. The numbers 1, 2, 3 etc., correspond to the percent of Schmidt net area divisions shown as abscissae in Figure 13. The lines (a) and (b) apply to the unshocked and shocked Coconino sandstone, respectively. The heavy line is the boundary which almost perfectly separates cumulative plots of non-shocked and shocked specimens, which, in general, also follow the descending order of Table 2.

are also slow, with a minimum of rotational components. Mylonitization processes are usually one-dimensional and relatively fast, with considerable rotation; but they occur at low pressures roughly equal to the shear strength of the rocks. The agencies of regional metamorphism which form gneisses, on the other hand, are long-acting, of low or high pressures depending on overburden, and are accompanied by shearing forces which act through large volumes and are variable with time and direction. The pressure environments produced by impacts are very rapid in development and impose pressures high enough to overcome the compressive, tensile, and shear strengths of both the massive rock and very often of its constituent minerals; in so doing shock processes become three dimensional and produce rotational tendencies. Furthermore, the attenuating rarefaction and compression waves impose additional opportunities for relative rotation of neighboring fragments.

An effective method of presenting the data is shown in Figure 14, where the cumulative number of grains displaying optic axis dispersal of a certain area or smaller is plotted against the area class. This diagram is based on the presentation of Dachille, Fauth, and Vand (1964). Results for unshocked and shocked Coconino sandstone (marked (a) and (b) in Fig. 14) indicate limits of plots obtained for the samples listed in Table 2. The heavy line between them is the boundary traced between plots of the two groups as separated by median and average rank in Table 2. The boundary is not perfect, because the upper parts of the plots for specimens of thermally metamorphosed sandstone and Fordham gneiss veered into high-area values. Nevertheless, points plotting well to the left or right of this boundary would strongly indicate a non-impact or impact history, respectively. For data plotting close to the boundary, curves with median values greater than that of the boundary would indicate an impact origin, particularly if the middle half of the cumulative curve were also to the right of the boundary.

In Figure 15 are shown the similar results from optic axis measurements of quartz grains in granodiorite from the Hardhat nuclear explosion site. The plots for the 13 kb and 32 kb locations practically coincide, as do those for 40 kb and 60 kb specimens. Unfortunately, thin sections of material exposed to higher pressures were not available at this time. However, sections of equivalent rocks from the Sedan cratering shot, subjected to shock pressures in excess of 150 kb, were examined and the results are also plotted. When compared with the boundary curve of Figure 14, cumulative curves for the Hardhat and Sedan specimens fall well to the right in the "shocked" area. By contrast, the curve of highly-deformed mylonite lies in the non-shocked side, well to the left of the boundary. Figure 15 demonstrates the potential utility of optic axis measurements in the field of shock metamorphism.

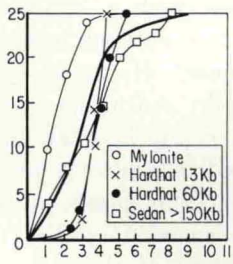

Fig. 15. Cumulative curves of quartz optic axis dispersion data of samples from the Hardhat and Sedan nuclear explosions, contrasted with data for a mylonite. The heavy line indicates the boundary discussed in Figure 14.

LASER ILLUMINATION OBSERVATIONS

A low intensity gas laser beam[2] was used as a convenient light source for illuminating small slabs or single crystals from various rock specimens. The crystals were immersed in oil and viewed under a microscope at right angles to the laser beam. The light reflected from the surfaces and the relatively few internal interfaces of ordinary undeformed crystals made them readily visible. However, highly shocked crystals, with their numerous internal interfaces, were invisible in a scintillating glow.

Furthermore, a beam impinging on a slab penetrated and illuminated an appreciable volume (approximately 1 cm^3) of unshocked, coarse-grained rocks and smaller volumes of fine-grained limestones. Highly-shocked rocks, notably Coconino sandstone from Meteor Crater, Arizona, contained and reflected the laser light within a hemisphere whose diameter was not much larger than that of the beam. These observations are consistent with the x-ray diffraction findings and may have bearing on a better understanding of the reflective properties of the lunar surface.

CONCLUSIONS

The x-ray and optical methods described, coupled with graphical representation of the data, are effective aids in revealing an impact history in any polycrystalline aggregate. These results are intimately related to internal fracturing of crystals on a submicroscopic scale, which is a dominant process in response to strong shock pressures and even to similar high pressures applied at the relatively slow rate of 5 kb/minute.

We gratefully acknowledge the support of the National Science Foundation with grant GP-4502. We are also indebted to several busy researchers for contributions of hard-to-get samples and we are happy to acknowledge here the assistance of Drs. R. S. Dietz, N. M. Short, T. E. Bunch, D. C. Gold, and T. C. Buschbach. To Professor V. Vand and to E. P. Meagher and J. Fauth go special thanks for many discussions and assistance at the beginning of these studies.

[2] Bausch and Lomb instrument; He–Ne continuous beam; 1 milliwatt rated power; 6328 A.

REFERENCES

Bailey, S. W., R. A. Bell, and C. J. Peng, Plastic deformation of quartz in nature, *Bull. Geol. Soc. Am., 69,* 1443–1466, 1958.

Chao, E. C. T., J. J. Fahey, J. Littler, and D. J. Milton, Stishovite, SiO_2 a very high pressure new mineral from Meteor Crater, Arizona, *J. Geophys. Res., 67,* 419–421, 1962.

Chao, E. C. T., E. M. Shoemaker, and B. M. Madsen, First natural occurrence of coesite, *Science, 132,* 220–222, 1960.

Dachille, F., Interactions of the earth with very large meteorites, *Bull. S.C. Acad. Sci., 24,* 1–19, 1962.

Dachille, F., J. Fauth, and V. Vand, Mechanical deformation of shocked quartz grains as determined by optic axis measurements (Abs.) *Geol. Soc. Am. Spec. Paper 82,* 39–40, 1964.

Dachille, F., E. P. Meagher, and V. Vand, Shock-induced polymorphism or alteration in minerals (Abs.), *Geol. Soc. Am. Spec. Paper 82,* 40, 1964.

Dachille, F., and R. Roy, Effectiveness of shearing stresses in accelerating solid phase reactions at low temperatures and high pressures, *J. Geol., 72,* 243–247, 1964.

Dachille, F., R. J. Zeto, and R. Roy, Coesite and stishovite: stepwise reversal transformations, *Science, 140,* 991–993, 1963.

Dawson, T. H., and M. F. Rose, X-ray diffraction studies on nickel after shock loading, *U.S. Naval Weapons Laboratory Report No. 1889,* 7 p., 1963.

Freeberg, Jacquelyn H., Terrestrial impact structures—a bibliography, *U.S. Geol. Surv. Bull. 1220,* 91 p., 1966.

Gigl, P., and F. Dachille, Effects of pressure and temperature on the reversal transitions of stishovite. (Abs.), *Meteoritics, 3,* 111–112, 1967.

Guinier, A., *X-Ray Crystallographic Technology,* London, Hilger and Watts Ltd., 330 p. 1952.

Myers, M. B., F. Dachille, and R. Roy, Pressure multiplication effects in opposed-anvil configurations, *Rev. Sci. Instr., 34,* 401–402, 1963.

O'Connell, Edna, A catalog of meteorite craters and related features with a guide to the literature, Rand Corporation, Santa Monica, Calif., Publication P-3087, 218 p., 1965.

Short, N. M., A comparison of features characteristic of nuclear explosion craters and astroblemes, *Ann. N.Y. Acad. Sci., 123,* 573–616, 1965.

Short, N. M., Effects of shock pressures from a nuclear explosion on mechanical and optical properties of granodiorite, *J. Geophys. Res., 71,* 1195–1215, 1966.

Skinner, Brian J., and J. J. Fahey, Observations on the inversion of stishovite to silica glass, *J. Geophys. Res., 68,* 5595–5604, 1963.